Investigation of Damage Properties of Woven Carbon-Epoxy Composites Modified with CNT Fillers

Mehmet Karahan* and Nevin Karahan

University of Bursa Uludag, Vocational School of Technical Science, Gorukle Bursa Turkey

Abstract: CNT/CNF grafting at high amount causes a CNT forest around the fiber and this causes significant limitations in composite material production. Due to increased distance between the fibers, local fiber volume fraction decreases within the yarns. Fiber volume fraction was found to decrease by 2.7–6.2% according to CNT/CNF ratio. The results revealed that there were significant decreases in mechanical properties and characteristic strain values where damage initiation and progression of the composite samples produced from carbon nanotubes grown on fabrics. It was found that Young's modulus values decreased by 15–17%. Characteristic strain values where damage threshold decreased by 36–53%. It was concluded that decreased local fiber volume fraction and low fiber-matrix interface bonding were the main cause for this situation. Moreover, it is believed that the one of the most important factor that might cause these limitations is lack of adequate wetting of fiber surfaces and low fiber-matrix interface bonding.

Keywords: CNT/CNF, Mechanical properties, Damage, Acoustic emission.

1. INTRODUCTION

The use of carbon nanotubes/nanofibers (CNT/CNF) in conventional fiber reinforced composite materials have significantly increased in recent years. The most common application in this subject involves using the CNT by mixing them in matrix resin at a certain ratio. Although this process is easy and fast, adding CNT significantly increases viscosity of resin and therefore makes production of composites difficult. As a result, adding CNT into the resin can only be performed at rather low ratios like 0.1-0.5% in practice. However, even at these low ratios, it was reported that inter-laminar shear strength of the composite structure improved by 69% and fracture toughness decreased by approximately 25% [1-7]. In case of CNT addition into resin increased viscosity of resin is not the only problem, tendency of easy agglomeration of CNTs is also a significant problem. This causes non-homogenous distribution of CNT in the structure and thus leads to the formation of weak spots in the structure. On the other hand, it can be possible to produce composite plates at desired quality level by cautiously controlling the conditions during production.

The fact that the CNTs develop very high mechanical properties at abovementioned levels even at low ratios is really interesting. However, it is a fact that high ratios cannot be achieved by mixing CNTs into resin. When CNTs are grown on fabric or fibers, it is possible to reach relatively higher CNT ratios [8-10]. CNT grown on fabric can be later used to produce the composite plates through RTM or autoclave methods. Since the CNTs on the fabric will not cause a problem like increasing resin viscosity, they will clearly show a more homogenous distribution. By growing CNTs on fabric, it is possible to reach high ratios like 10%. However, potential problems during production of composite at high CNT ratios using such a technique remain unknown.

Almost many of the studies on CNT reinforced composites concentrated on inter-laminar shear strength, fracture toughness and fiber-matrix interface bonding strength [1-7]. On the other hand, the studies on how adding CNT affects damage initiation and progress generally analyzed composite materials where CNTs are mixed or dispersed to the resin [9-13]. In CNT grown on composites, the effect of CNTs on damage initiation and propagation was not analyzed.

This study examined basic mechanical properties with damage initiation and propagation properties of composite plates produced with CNT grown on 2x2 twill woven carbon fabric and compared the results without CNT or virgin plates. The study focuses on static tensile tests carried out along the fiber direction that are accompanied by acoustic emission (AE) registration and full-field strain measurements.

2. MATERIALS AND TEST METHODS

Parameters and the surface view of the fabric, chosen as the baseline material and a substrate for growth of CNT, are shown in Table **1** and Figure **1.** The geometric aspects of the fabric structure were identified

*Address correspondence to this author at the University of Bursa Uludag, Vocational School of Technical Science, Gorukle Bursa Turkey;
Tel: +905323666464; E-mail: mkarahan@uludag.edu.tr

E-ISSN: 2311-8792/22

in [14]. The size of the substrate used for growth of CNT is limited by the dimensions of the reactor. Therefore, the fabric was cut into strips with the size approximately 5x25 cm. These strips were handled with all the possible care, as the twill fabric is easily deformed.

The CNT were grown using the proprietary knowledge of company Nanocyl. The process parameters used to grow CNT on the fabric samples were from the standard production process of multiwall CNT of Nanocyl. Time, temperature and flow rate of gases was very important in controlling the homogeneity, level (wt%), and length of CNT on the fabric surface. First, the fabric sample is heated up to 300°C to remove the sizing from the carbon fibers. Then the sample is immersed in the ethanol solvent of the catalyst (Ni(NO3)2.6H2O). The concentration of the catalyst, the synthesis time, the flow gas rate of acetylene and hydrogen depends on the desired amount of CNT growth. The resulting amount of the catalyst particles (size of several nanometers) on the carbon fibers is estimated as about 6 mg of Ni per 1 g of carbon for 8 to 10 wt% CNT growth and about 2 mg of Ni per 1 g of carbon for the 2 to 4 wt% CNT growth (the weight percents in relation to the weight of the fabric). The sample is dried at 120°C during 1 hour and placed in the CNT-growth reactor. A flow of acetylene, hydrogen and nitrogen (respectively 1/0.5/1 ratio) passed through the 600°C heated reactor during 90 seconds. The average diameter of such a MWCNT is 9.5 nm, number of walls 5… 10, the length depends on the growth time.

Two batches of the CNT-grafted fabric samples were produced (Table **2**). The values of the amount of CNT on the fabric samples were determined by weighing of the samples before and after the processing.

Table 1: Parameters of Carbon Woven Fabric (G986)

Weave	Twill 2/2
Warp/Weft yarns	6K HTA carbon fiber
Ends/Pick counts, yarns/cm	3.5
Weight, gr/m^2	285
Fiber diameter, μm	7

The size of the fabric strips used for growth of CNT is limited by the dimensions of the reactors in the labs. Therefore 25 mm wide fabrics were used to produce the composite samples. Shell epoxy resin Epikote 828 LV and the hardener Epikure DX 6514 were used as the matrix. The composite plates were produced by using vacuum-assisted resin transfer molding (VARTM) equipment with 5 plies of fabric to obtain a fiber volume fraction of 52% and a thickness of approximately 1.5 mm. For comparison, the results of a previous study [15] obtained from sample produced with same fabric, resin and lab conditions but without CNT were used.

Before placement of the fabrics, the mould cavity was warmed to 40ºC to reduce resin viscosity and hence the cycle time. The fabric was stacked in the mould cavity in the warp direction. After degassing, the resin was injected into the mould cavity at a pressure of 2 bars for 2 min. Then the pressure was increased, up to 4–5 bars, until the cavity was filled. As the cavity was filled, the resin flow was maintained as long as possible, allowing the resin flow to fill the voids. Subsequently, the vacuum port, where the resin was stored in the mould, was closed, and a packing pressure of 5 bars was applied. This post-fill action was necessary to minimize voids in the plate. After injection, the mould was heated to 70ºC for 1 h to cure the resin. The composite plate was post-cured in the mould at 160ºC for 2 h. The mould was then cooled to 40ºC. Main production parameters were given in Table **2**.

Tensile tests were performed on an Instron 4505 testing machine with a crosshead speed of 5 mm/min. The 20x210 mm samples were cut out of the composite panels in the warp direction using a diamond saw. Glass/epoxy composite tabs were stuck to the ends of the samples using epoxy resin. The specimen length between the tabs was 120 mm.

A LIMESS camera took images of the black and white painted region at a frequency of 2 Hz. The first image, which was taken as soon as the test started, showed the non-deformed stage. The local displacement and strain data were established by comparing subsequent images to the first image with Vic2D software (LIMESS Messtechnik und Software GmbH) [13, 14].

Two AE sensors which were placed at the boundaries of the gauge length region allowed to listen each AE event to be recorded to relate energy and the corresponding applied load. Signals that occurred outside of the sensors were filtered out by the AE system AMSY-5 by using a suitable calibration procedure. In the course of the experiment, the energy of AE events was registered and the cumulative energy of AE events was followed as function of applied tensile strain. Changes of rate of generation of AE events, reflected by the change of slope of the diagram,

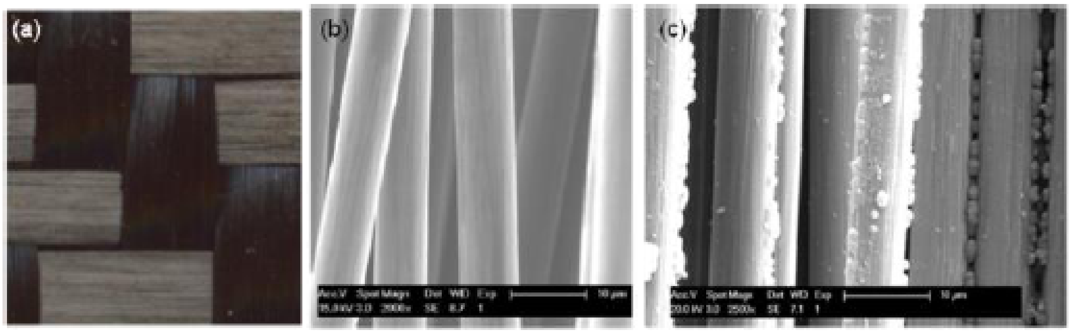

Figure 1: Surface view of the fabric (**a**) and SEM micrographs of carbon fibres inside the fabric: (**b**) without (Sample **A**) and (**c**) with CNT grown on the fabric (Sample **B**).

indicate change in damage mechanisms in the sample. Since the AE sensors are very sensitive, they had to be removed before the final failure of the sample. This made it impossible to study the very last stage of damage development. As a result of these tests, the ultimate stress and strain values were determined. Also, characteristic damage threshold strain values (ε_{min}, ε_1 and ε_2), were determined with the help of the AE records: ε_{min}, at which the first AE event occurred; ε_1, first damage initiation; ε_2 second damage initiation stage. Several samples were cross-sectioned and polished, and the crack and damage patterns were studied with an optical microscope.

3. RESULTS AND DISCUSSIONS

3.1. Mechanical Properties

Unexpected results were obtained from identification of thickness and fiber volume fraction of composite plates which are produced according to VARTM method. Despite using fabrics having the same amount of layers and using mould at the same thickness in VARTM method, it was found that nano fiber reinforced composite (nFRC) plates were thicker than virgin plates (Table **2**). Thickness increased by 3.9-7.9% depending on CNT ratio. On the other hand, fiber volume fraction decreased by 2.7-6.2%. Although the difference was not so high, it was observed that thickness of plates increased as well. Increased plate thickness is caused by the CNTs around the fibers. The CNTs around fibers increase the distance between the fibers. This also affects compressibility of fibers during RTM process. Due to high RTM pressure, thickness cannot vary during the production of composite plates. The final thickness of the plate is defined by the spacer thickness and by relaxation of the plate after the mould is open, which, in its turn, depends on cure shrinkage of the matrix, which is affected by the presence of CNTs.

Due to CNT layer around fiber, the fiber diameter increases and therefore compressibility in mould during resin injection becomes difficult. As a result of this, thickness of the produced composite plate increases, which causes decreasing of fiber volume fraction locally within the composite [8]. This is an important limitation that should be taken into account in production of nFRC. Because it should not be ignored that mechanical properties will also decrease depending on decreased fiber volume fraction of composite. A similar problem occurred even in carbon epoxy composite plates where the CNTs produced with the same fabric and resin are mixed or dispersed with resin [18].

Local fiber volume fraction decreases depending on increased diameter or increased distances due to the CNTs in around the fibers. This will clearly cause a significant decrease in mechanical properties and damage initiation properties of composite material [15].

These values are computed over the initial range (strain up to 0.1%), the middle range (strain between 0.1% and 0.3%), and the upper range (strain between 0.3 and 0.6). The Young's modulus values have been determined from the stress and strain data for equal length strain intervals (ε_a, ε_b) using equation $E=(\sigma_b-\sigma_a)/(\varepsilon_b-\varepsilon_a)$.

Characteristics of the stress-strain curve were not affected by variations in fibre volume fractions; the same trends were seen for all samples. In addition, the Young's modulus gradually decreased as strain increased for all fibre volume fractions tested. The Young's modulus increased monolithically depending on the increase in fibre volume fraction. Figure **2d** shows initial Young's modulus values for 3 different samples.

Table 2: Fibre Volume Fraction Values Obtained for Plates Manufactured with Different Fabric Ply Numbers and Thicknesses

Sample	% Weight of Ratio of CNT on the Fabric	Fabric Ply Number in the Composite	Plate Thickness, mm	Fiber Volume Fraction (V_f), %
A [12]	0	5	1.52±0.008	52±0.27
B	2-4±0.6	5	1.58±0.012	50.6±0.24
C	7-11±1.0	5	1.64±0.016	48.8±0.33

Table 3: Experimentally Determined Mechanical Properties of the Woven Carbon-epoxy Composites in the Warp Direction

Parameter	Samples								
	Reference-Sample A			Sample B			Sample C		
	Average	Std.dev	% CV	Average	Std.dev.	% CV	Average	Std.dev	% CV
E (0 - 0.1%), GPa	64.74	6.78	*10.4*	58.50	4.82	*8.3*	54.40	5.24	*9.6*
E (0.1 - 0.3%), GPa	63.42	7.64	*12.0*	57.26	6.21	*10.8*	52.13	3.05	*5.8*
E (0.3 – 0.6%), GPa	61.87	10.2	*16.4*	55.76	4.50	*8.0*	48.31	5.21	*10.8*
Poisson ratio	0.26	0.10	*38.4*	0.26	0.14	*38.4*	0.24	0.03	*42.6*
σ_{ult}, MPa	702	12	*1.7*	613	10.5	*1.7*	562	9	*1.6*
ε_{ult}, %	1.13	0.01	*0.9*	1.105	0.02	*1.8*	1.02	0.01	*1.1*
ε_{min}, %	0.19	0.02	*12.0*	0.11	0.01	*9.1*	0.088	0.01	*11.3*
ε_1, %	0.26	0.02	*6.0*	0.16	0.02	*12.5*	0.13	0.01	*7.7*
ε_2, %	0.30	0.02	*5.0*	0.19	0.02	*10.5*	0.17	0.01	*5.8*

Tensile test results of the nFRC and virgin samples are comparatively presented in Table **3**. The results were obtained contrary to the expectations and the mechanical properties of nFRC plates showed a significant decrease rather than increase. In addition to the decrease in elastic properties, damage threshold properties decreased as well.

Table **3** shows 3 different values of the Young's modulus for each of the samples due to the non-linearity of the stress-strain curves. These values are computed over the initial range (strain up to 0.1%), the middle range (strain between 0.1% and 0.3%), and the upper range (strain between 0.3 and 0.6). The Young's modulus values have been determined from the stress and strain data for equal length strain intervals (ε_a, ε_b) using equation $E=(\sigma_b-\sigma_a)/(\varepsilon_b-\varepsilon_a)$.

The initial Young's modulus was 64.74 GPa for the composite sample A. Young's modulus decreased by 1.32 GPa (or 2%) between 0.1% and 0.3% strain. Although the decrease was low within this range, it increased after 0.3% strain. The Young's modulus decreased by 2.87 GPa (or 4.5%) within the range of 0.3% - 0.6%. A decrease of approximately 25% in the Young's modulus occurred from the beginning of the test until the ultimate failure (Figure **2a**). The initial Young's modulus was 58.5 GPa for the composite sample B. A. Young's modulus decreased by 1.24 GPa (or 2.1%) between 0.1% and 0.3% strain. The Young's modulus decreased by 2.74 GPa (or 4.6%) within the range of 0.3% - 0.6%. A decrease of approximately 32% in the Young's modulus occurred from the beginning of the test until the ultimate failure (Figure **2b**). This indicated the damage propagated as significantly for nFRC plates after a certain value of strain. The initial Young's modulus was 54.4 GPa for the composite sample C. A. Young's modulus decreased by 2.27 GPa (or 4.2%) between 0.1% and 0.3% strain. The Young's modulus decreased by 6.09 GPa (or 11.2%) within the range of 0.3% - 0.6%. A decrease of approximately 36% in the Young's modulus occurred from the beginning of the test until the ultimate failure (Figure **2c**).

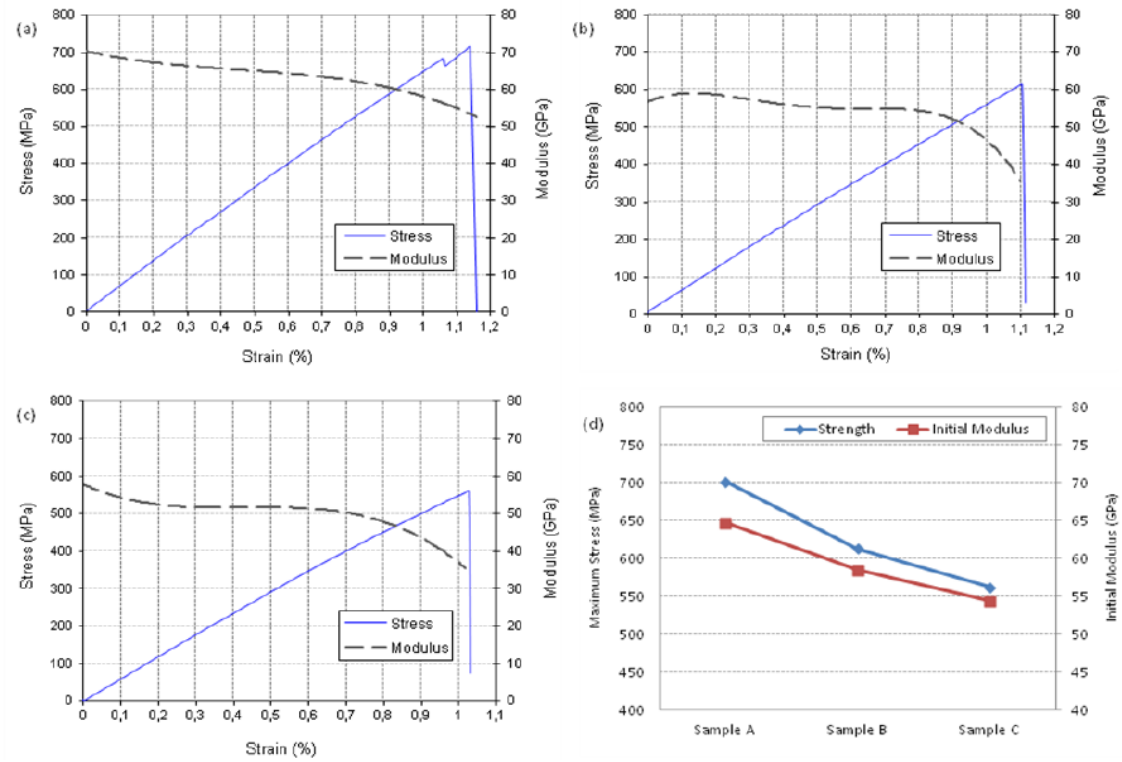

Figure 2: Stress-strain and module-strain variations in composite materials: (**a**) Sample A [12]; (**b**) Sample B; (**c**) Sample C; (**d**) Changing of Maximum stress and Initial Young's module.

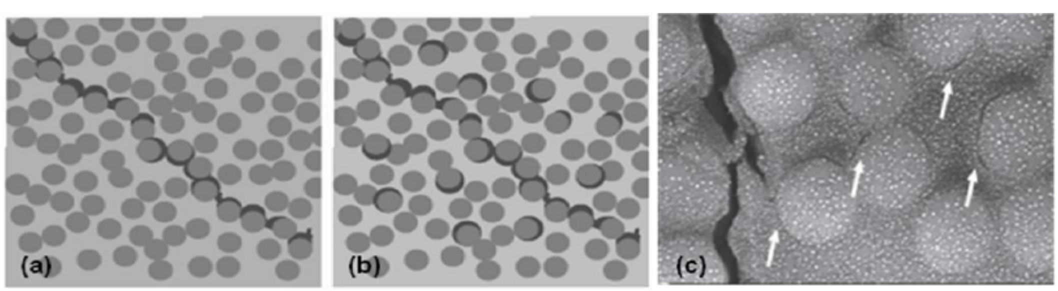

Figure 3: Schematics of a mechanism for crack formation inthe virgin composite (**a**) and nFRC (**b**): (**a**) a crack path is formed along the tranversal direction in virgin composite; (**b**) a crack and multiple debonding sites in nFRC composite; (**c**) SEM image of transversal cracks and fiber-matrix debondings in nFRC composite [18].

Comparison of the results showed that Young's modulus value decreased by 14% on average for Sample B while it decreased by 18% on average for Sample C according to the Sample A. The same thing was also valid for tensile strength. In tensile strength values, for Sample B there was 21% decrease on average according to reference sample and for Sample C there was a decrease of 18% on average. Ultimate strain values were 15% low for Sample B and 17% low for Sample C according to Sample A.

Stress-strain diagrams given in Figure **2** shows that they are almost linear to a certain value. However, after a certain value, the curve shows a non-linear behavior. This is caused by the decrease of modulus depending on damage progress in composite structure and modulus-strain curves support this view. The non-linear region in the curve is thought to be the region where damage significantly progressed and this will be discussed in the following section.

The decrease in mechanical properties due to CNT on the fibers is rather strange. It was found that adding CNT to resin generally improved mechanical properties, particularly in fracture toughness [1-7]. With this method, it is possible to add CNT to the resin at rather low ratios however even this have significant limitations. For example: excessive thickening of the resin and agglomeration. CNT grown on fibers makes high amounts of CNT addition in composite structure possible. However, it was found that stiffness values of composites significantly decreases (14-18%) with this method. This is believed to have two reasons. The first reason is reduced local fiber volume fraction. This occurred due to increased distance between the fibers and fiber volume fraction has a direct effect on mechanical properties. Lower fiber-matrix interface bonding is thought to be the second factor. CNT layer around the fiber makes it difficult for the resin to sufficiently wet the fiber. Damage images obtained from SEM analyses obtained in another study which used the same fabric and resin support this view (Figure **3**) [18]. In the mentioned study it was observed that the cracks in a virgin composite plate which without CNT showed a more brittle structure character and damage progressed through the propagation of transversal cracks; while in composite plates with CNT, the cracks were first initiated as individual fiber-matrix interface and then these cracks combined and turned into transversal cracks [18]. Apart from previous studies, we worked with much higher ratios of CNT in the present study and in microscope analyses on the tested samples it was observed that there were debonding not only in fiber-matrix but also in yarn-matrix boundaries. This is caused by inadequate wetting of the fibers and therefore a weak fiber-matrix interface bonding. A considerable amount of CNT layer forms around the fibers and this layer makes penetration of resin to fibers. This causes weak fiber-matrix interface and makes the damage to progress easily.

Results of a previous study which added low ratios of CNT into resin [18] contain highly comparable data with the present study. In a previous study [18], it was reported that adding CNT into 0.25% CNT reinforced composite plates produced with the same fabric, resin and laboratory conditions did not cause a change in Young's modulus however caused a slight increase in resistance value. Increased CNT ratio caused significant decreases in mechanical properties and Young's modulus. This indicates that there is a sufficient limitation in composite materials produced by adding CNT.

3.2. Damage Investigations

Damage initiation and development in the composite samples was characterized by monitoring acoustic emissions (AE) during the test, as well as by microscopically examinations.

Table **3** shows characteristic strain levels for damage initiation and propagation in samples having different fibre volume fractions. Figure **4** shows AE measurements with the average stress-strain curve for the composite samples.

AE records showed highly similar trend for all three samples. For the reference sample (Sample A) ε_{min}, $\varepsilon_1$and ε_2 were determined as 0.19 (stress about 130 MPa), 0.26 (stress about 180 MPa) and 0.30 (stress about 205 MPa) respectively [15]. For Sample B ε_{min}, $\varepsilon_1$and $\varepsilon_2$were found to be 0.11% (stress about 65 MPa), 0.16% (stress about 90 MPa) and 0.19% (stress about 105 MPa) respectively. For Sample C, ε_{min}, $\varepsilon_1$and $\varepsilon_2$were found to be 0.088% (stress about 45 MPa), 0.13% (stress about 70 MPa) and 0.17% (stress about 90 MPa) respectively. Characteristic strain values for damage initiation and development are comparatively presented in Figure **4**. Based on these results, according to reference sample, for Sample B, ε_{min}, ε_1 and ε_2 decreased by 42%, 38% and 36% respectively and for Sample C, ε_{min}, ε_1 and ε_2 decreased by 53%, 50% and 43% respectively. These values indicate a dramatic decrease in damage initiation and propagation strain values. In some studies [18, 19] nFRC samples where produced with the same fabric, resin and laboratory conditions but CNT mixed to the resin, approximately 0.2% increase was reported in damage threshold strain values. These results revealed that CNT grafting method on fibers at high ratios have big limitations for composite properties.

Analysis of AE diagrams (Figure **4**) show that damage initiated much earlier and propagated much faster in nFRC samples than virgin sample. This indicates that transversal cracks rapidly propagate in the sample due to weak fiber-matrix interface. The cracks generally occur in fiber-matrix interface in nFRC samples and then propagate along the entire sample width. Transversal cracks cause a gradual decrease in stiffness of the material. Based on the analysis of the change in Young's modulus in Figure **2** it can be stated that the decrease in the modulus gradually and slowly decreased for the virgin sample depending on the increase in the amount of transversal cracks. However, in nFRC samples, this decrease rapidly occurred particularly after a certain level. This means increased transversal cracks and delamination in yarn boundaries and/or between the layers (Figure **5**).

Since the diagrams are prepared with the same scale, the difference between ε_1 and ε_2 values can be easily observed. In addition to early initiation of damage in nFRC samples, high-energy events take place quickly and the frequency of occurring events was higher than the virgin sample. Increase of cumulative energy level proves this phenomenon (Figure **4.c**). Damage progression after it initiated occurred earlier than the reference sample.

It is difficult to explain these unexpected results both in tensile properties and damage initiation and progress properties. However, as indicated in the present study, although CNT application has many advantages reported in the literature, there are low number of limitations as well. It is believed that these results probably have three main causes:

- High temperature is used during CNT grafting process on fibers and the sizing (coating material) on carbon fibers are fully removed during this process. The sizing has two important functions: the first one is to reduce friction of the fibers during weaving and production and to protect fiber breaking and the second one is to increase bonding with resin during composite production. When this material is completely removed from fiber surface, bonding with resin property of the fibers might be decreased and thus fiber-matrix interface resistance might be

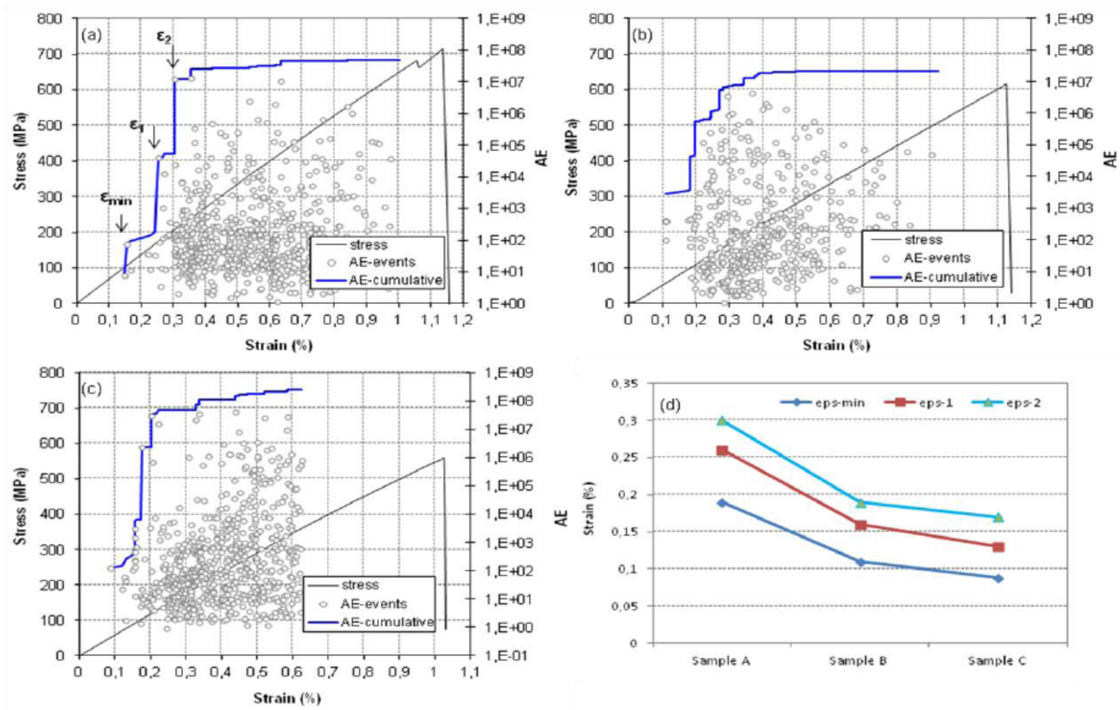

Figure 4: Acoustic emission monitoring of damage in different composite materials: (**a**) Sample A [15]; (**b**) Sample B; (**c**) Sample C. The graph shows a dependency on the applied strain of stress, energy of individual AE events and cumulative energy (arbitrary units). Values of ε_{min}, ε_1 and ε_2 indicate the damage thresholds; (**d**) Comparative view of the characteristic strain values for damage initiation and propagation for different samples (eps-min, eps-1 and eps-2 indicate the ε_{min}, ε_1 and ε_2 respectively).

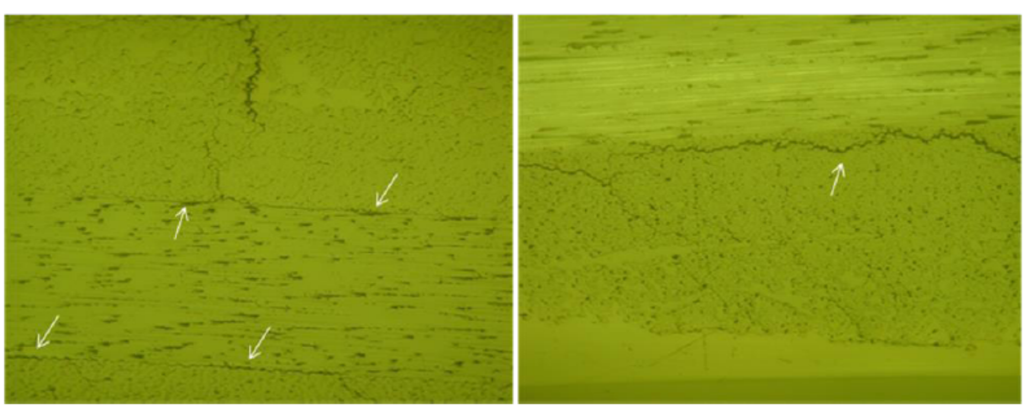

Figure 5: Delamination cracks between the yarn boundaries in nFRC samples. Arrows indicate the delamination cracks.

decreased. This can be a major factor for lower mechanical properties.

- The second important cause is that CNTs which are intensively placed on fiber surface prevent the fiber to be wetted by the resin and therefore fiber-matrix interface bonding decreased.
- The third cause can be that the CNTs increase the distance between the fibers and as a result, decrease fiber volume fraction. This can also cause a decrease in mechanical properties. However, damage initiation and progress strain levels is not affected from change of fiber volume fraction [15].

All of these three principle causes are believed to have a cumulative effect on decreased mechanical properties, damage initiation and progression properties. Unwetted fibers adequately by the resin and therefore decreased fiber-matrix interface bonding and decreased fiber volume fraction might have caused decrease in these properties.

4. CONCLUSIONS

This study examined the effect of CNT grafting on fibers on mechanical and damage threshold properties in nFRC materials. The results are presented below.

CNT grafting at high amount causes a CNT forest around the fiber [20] and this causes significant limitations in composite material production.

Due to increased distance between the fibers, local fiber volume fraction decreases within the yarns. Fiber volume fractions were found to decrease by 2.7-6.2% according to CNT ratio.

Significant decreases were observed in mechanical properties of nFRC samples. Young's modulus values were found to be decrease by 15-17%. It was concluded that decreased local fiber volume fraction and low fiber-matrix interface bonding was the main cause of this situation.

Damage threshold strain values globally decreased by 36-53%. It is believed that the most important factor that might cause this decrease is lack of adequate wetting of fiber surfaces and low fiber-matrix interface bonding.

The initial damage occurred at intersections of weft and warp yarns. At these locations, yarn crimps are at a maximal level. Fibre-matrix debonding began at the ε_{min} level. Transversal cracks first occurred at the ε_1 level; their sizes were restricted by the width of weft yarns. Cracks propagating across the sample occurred and further cracks were initiated at the ε_2 level.

REFERENCES

[1] Warrier, A., O. Rochez, A. Godara, L. Mezzo, F. Luizi, L. Gorbatikh, A. Van Vuure, SV. Lomov, and I. Verpoest. Surface modification of glass fibers with carbon nanotubes and their composites. in SEICO 09 - SAMPE EUROPE 30th. International Jubilee Conference and Forum. 2009. Paris.

[2] Garcia, EJ., BL. Wardle, and AJ. Hart, Joining prepreg composite interfaces with aligned carbon nanotubes. Composites Part A Applied Science and Manufacturing, 2008; 39(6): p. 1065-1070. https://doi.org/10.1016/j.compositesa.2008.03.011

[3] Blanco, J., EJ. Garcia, RG. De Villoria, and BL. Wardle, Limiting Mechanisms of Mode I Interlaminar Toughening of Composites Reinforced with Aligned Carbon Nanotubes. Journal of Composite Materials, 2009; 43(8): 825-841. https://doi.org/10.1177/0021998309102398

[4] De Riccardis, MF., D. Carbone, TD. Makris, R. Giorgi, N. Lisi, and E. Salernitano, Anchorage of carbon nanotubes grown on carbon fibres. Carbon, 2006; 44(4): 671-674. https://doi.org/10.1016/j.carbon.2005.09.024

[5] Garcia, EJ., AJ. Hart, and BL. Wardle, Long carbon nanotubes grown on the surface of fibers for hybrid composites. AIAA Journal, 2008; 46(6): 1405-1412. https://doi.org/10.2514/1.25004

[6] Garcia, EJ., BL. Wardle, AJ. Hart, and N. Yamamoto, Fabrication and multifunctional properties of a hybrid laminate with aligned carbon nanotubes grown In Situ. Composites Science and Technology, 2008; 68(9): 2034-2041. https://doi.org/10.1016/j.compscitech.2008.02.028

[7] Qian, H., A. Bismarck, ES. Greenhalgh, G. Kalinka, and MSP. Shaffer, Hierarchical composites reinforced with carbon nanotube grafted fibers: The potential assessed at the single fiber level. Chemistry of Materials, 2008; 20(5): 1862-1869. https://doi.org/10.1021/cm702782j

[8] Lomov, SV, Gorbatikh, L, Kotanjac, Z, Koissin, V, Houlle, M, Rochez, O, Karahan, M, Mezzo, L, Verpoest, I, Compressibility of carbon woven fabrics with carbon nanotubes/nanofibres grown on the fibres, Composites Science and Technology, 2011; 71: 315-325. https://doi.org/10.1016/j.compscitech.2010.11.024

[9] Lomov, S. V., Gorbatikh, L., Greef, N., Karahan, M., Godara, A., Mezzo, L., Luizi, F., Verpoest, I., Nano-engineered fibre reinforced composite: Gain in properties and limitations of the manufacturing, 14th European Conference on Composite Materials, 7-10 June 2010, Budapest, Hungary.

[10] Gorbatikh L., Ding Y., De Greef N., Ivanov D., Karahan M., Godara A., Mezzo L., Lomov SV., Verpoest I., Effect of Carbon Nanotubes on the Damage Development in Fiber Reinforced Composites, 14th European Conference on Composite Materials, 7-10 June 2010, Budapest, Hungary.

[11] Bilisik, K, Karaduman, NS, Sapanci, E. Flexural characterization of 3D prepreg/stitched carbon/epoxy/multiwall carbon nanotube preforms and composites. J Compos Mater 2019; 53: 563-577. https://doi.org/10.1177/0021998318787861

[12] Kashif, M, Hamdani, STA, Zubair, M, et al. Effect of interlocking pattern on short beam strength of 3D woven composites. J Compos Mater. 2019; 53: 2789-2799. https://doi.org/10.1177/0021998319839441

[13] Bilişik K, Karaduman N, Sapancı E, Short-Beam Shear Nanopreg/nanostitched Three-Dimensional Carbon-Epoxy

Multiwall Carbon Nanotube Composites, Journal Of Composite Materials, 2020; 5(3): 311-329 https://doi.org/10.1177/0021998319863472

[14] Karahan, M., Lomov S., V., Bogdanovich, AE., Mungalov, D., Verpoest, I., Internal geometry evaluation of non-crimp 3D orthogonal woven carbon fabric composite, Composites Part A, 2010; 41: 1301-1311. https://doi.org/10.1016/j.compositesa.2010.05.014

[15] Karahan M, The effect of fibre volume fraction on damage initiation and propagation of woven carbon-epoxy multi-layer composites, Textile Research Journal, 2011; 82(1): 45-62. https://doi.org/10.1177/0040517511416282

[16] Karahan M, Investigation of damage initiation and propagation in 2x2 twill woven carbon-epoxy multi-layer composites, Textile Research Journal, 2011; 81(4): 412-428. https://doi.org/10.1177/0040517510395996

[17] Lomov, SV., Bogdanovich, AE., Ivanov, DS., Mungalov, D., Karahan, M., Verpoest, I., A comparative study of tensile properties of non-crimp 3d orthogonal weave and multi-layer plain weave e-glass composites. Part 1: materials, methods and principal results, Composites A, 2009; 40: 1134-1143. https://doi.org/10.1016/j.compositesa.2009.03.012

[18] De Greef N, Gorbatikh L, Godara A, Mezzo L, Lomov SV, Verpoest I, The effect of carbon nanotubes on the damage developmentin carbon fiber/epoxy composites, Carbon, 2011; 49: 4650-4664. https://doi.org/10.1016/j.carbon.2011.06.047

[19] Gorbatikh L, Ding Y, De Greef N, Ivanov D, Karahan M, Godara A, Mezzo L, Lomov SV, Verpoest I, Effect of carbon nanotubes on the damage development in fier-reinforced composites, 14th European Conference on Composite Materials 7-10 June 2010, Budapest, Hungary Paper ID: 837-ECCM14.

[20] Lomov SV, Koissin V, Karahan M, Godara A, Gorbatikh L, Verpoest I. Compressibility of CNT-grafted fibrous reinforcements: a theory. International Journal of Material Forming, 2010; 3: 627-30. https://doi.org/10.1007/s12289-010-0848-3

Received on 15-03-2022 Accepted on 10-04-2022 Published on 28-04-2022

DOI: http://dx.doi.org/10.12974/2311-8792.2022.08.1